DEMUX OPERATION IN TANDEM AMORPHOUS SI-C DEVICES
A two stage active circuit

M. A. Vieira[1,2] , M. Vieira[1,2,3] , P. Louro[1,2] , A. Fantoni[1,2] and A. Garção[2,3]

[1] *Electronics Telecommunications and Computer Dept, ISEL, Lisbon, Portugal*
[2] *CTS-UNINOVA, Lisbon, Portugal*
[3] *DEE, FCT-UNL, Lisbon, Portugal*

Abstract: Characteristics of tunable wavelength filters based on a-SiC:H multilayered stacked cells are studied both theoretically and experimentally. Curves of gain vs. wavelength illustrate the optical filter characteristics. A capacitive active band-pass filter model supports experimental data. Results show that the use of a double pi'n/pin a-SiC:H heterostructure as active capacitive filters depends on the wavelength and modulated frequency of the trigger light and on the wavelength of the additional optical bias. The devices combine three indispensable functions of transceivers, amplification, detection and wavelength filtering. Experimental and simulated results show the device combines the properties of active short-pass and long-pass filter sections into a capacitive active band-pass filter.

1   INTRODUCTION

The deployment of Fiber to the Home (FTTH) access networks and the emergence of Optical Network installations leads to a need for mass production of bi-directional optical modules that can exchange data up- and downstream through a single fiber. In order to reduce the cost per user connected to the network, production cost of the optical modules at the optical network unit must be exceptionally low [1, 2]. Amorphous silicon carbon tandem structures, through an adequate engineering design of the multiple layers' thickness, absorption coefficient and dark conductivities can accomplish this function. Here, we propose photodiodes with integrated optical thin film filters reducing module cost by minimizing the number of discrete filters.

Since filters are defined by their wavelength-domain effects on signals, it makes sense that the most useful analytical and graphical descriptions of filters also fall into the wavelength domain. Knowing the transfer function magnitude (or gain) at each wavelength allows us to determine how well the optical filter can distinguish between signals at different wavelengths. Typical wavelengths used in infrared optical network transceivers are long wavelengths for downstream data and short wavelengths for upstream communication. In this study we demonstrate the subsequently opportunity integration of two useful optical active filters, a short-and a long-pass filter, eliminating crosstalk between downstream and upstream channels transceivers, by transmitting only one of the two datastreams and blocking the other: red channel and/or green channel for downstream data and blue channel for upstream data.

In this paper we demonstrate the integration of short-pass and long-pass optical thin film filters targeting applications combined with a versatile amorphous Si/SiC p-i'-n-p-i-n device concept.

2   EXPERIMENTAL DETAILS

2.1   Device optimization and operation

Voltage and optical bias controlled devices, with front and back indium tin oxide transparent contacts, were produced by PECVD at 13.56 MHz radio frequency and tested for a proper fine tuning of the visible spectrum.
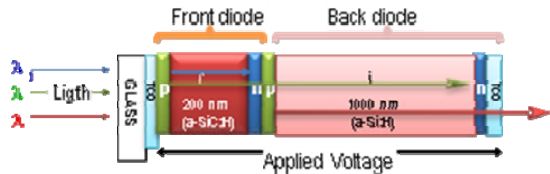
Figure1   Device Configuration

The active device (Fig. 1), consists of a p-i'(a-SiC:H)-n/p-i(a-Si:H)-n heterostructure with low conductivity doped layers ($<10^{-7}\Omega^{-1}cm^{-1}$). The thicknesses and optical gap of the thin i'- (200nm; 2.1 eV) and thick i- (1000nm; 1.8eV) layers are optimized for light absorption in the blue and red ranges, respectively [3]. Transparent contacts have been deposited on front and back layers to allow the entrance and exit off of the light from both sides.

Photo generation occurs firstly in the a-SiC:H absorber, and the remaining non-absorbed light goes through the a-Si:H layer. As result, both front and back diodes act as optical filters confining, respectively, the blue and the red optical carriers, while the green ones are absorbed across both [4].

The device operates within the visible range using as input color channels (data) the modulated light (external regulation of frequency and intensity) supplied by a red (R: 626 nm; 51µW/cm²), a green (G: 524 nm; 73µW/cm²) and a blue (B: 470nm; 115µW/cm²) LED. Additionally, steady state red, green and blue illumination (background) was superimposed using similar LEDs. Light was always impinging from the glass side.

2.2   Transfer function characteristics

Spectral response measurements and transfer function magnitude (gain) characteristics at different frequencies (250Hz-3500Hz) were analyzed. The spectral sensitivity was tested through data transmission measurements under different frequencies, with and without applied steady state bias.

In Fig. 2, the spectral photocurrent of the stacked device (Fig.1), at 250Hz, is displayed under red, green and blue background irradiations (color symbols) and without it (black symbols). For comparison the normalized spectral photocurrent for

the front, p-i'-n, and the back, p-i-n, photodiodes (lines) are superimposed. Data confirm that the front and back photodiodes act, separately, as optical filters. Each diode, separately, presents the typical response of single p-i-n cells with intrinsic layers based on a-SiC:H or a-Si:H materials, respectively. The front diode, based on a-SiC:H heterostructure, cuts the wavelengths higher than 550nm while the back one, based on a-Si:H, cuts the ones lower than 500nm. Results show that the background wavelength has a strong influence on the spectral sensitivity of the all device.
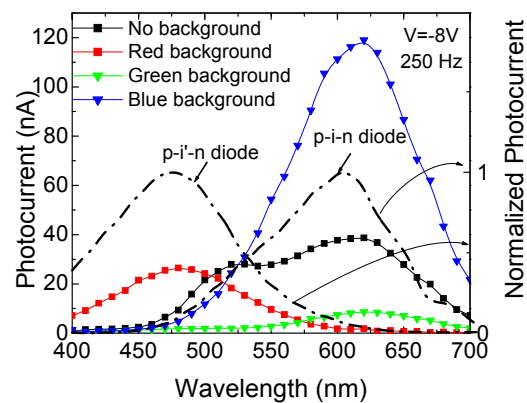
Figure 2   Spectral photocurrent without and under different background wavelengths (symbols).The normalized spectral current for the front, p-i'-n, and the back p-i-n photodiodes separately (lines) is superimposed.

Under red irradiation, when compared with its value without external background, the photocurrent is strongly enhanced at short wavelengths and disappears for wavelengths higher than 550 nm, acting as a short-pass filter. Under blue irradiation the devices behaves as a long-pass filter for wavelengths higher than 550 nm, blocking the shorter wavelengths.

In Fig. 3 the spectral gain, defined as the ratio between the spectral photocurrents, under red (α^R), green (α^G) and blue (α^B) steady state illumination and without it (no background) are plotted at 250Hz (lines). Under green background it is also displayed the spectral photocurrent at 3500Hz (symbols).

Results from both Fig. 2 and Fig. 3 confirm the wavelength controlled spectral sensitivity of the device, under steady state illumination. Under green irradiation the spectral response depends on the frequency. At 250Hz the spectral sensitivity is strongly reduced while at 3500Hz the device behaves as a band-stop active filter that screens out the medium wavelength range (green) enhancing

only the photocurrent for wavelengths outside of that range.
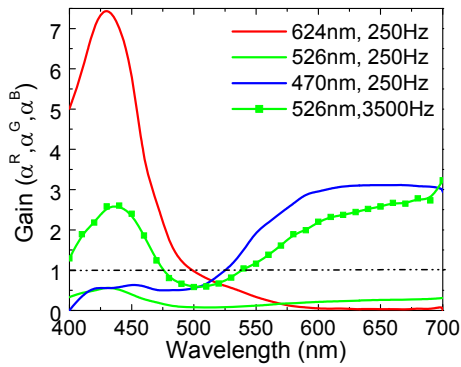
Figure 3   Spectral gain under red (α^R), green (α^G), and blue (α^B), optical bias for different frequencies.

When an external bias is applied to a double pin structure, its main influence is in the field distribution within the less photo excited sub-cell [4]: the front cell under red irradiation; the back cell under blue light, and both, under green steady state illumination (Fig. 1). In comparison with thermodynamic equilibrium conditions (no background), the electrical field under illumination is lowered in the most absorbing cell (self forward bias effect) while the less absorbing reacts by assuming a reverse bias configuration (self reverse bias effect). So, the sensor is a bias wavelength current-controlled device that makes use of changes in the wavelength of the background to control the power delivered to the load, acting as an optical amplifier. Its gain (Fig. 3) depends on the background illumination wavelength. If the electrical field increases locally (self optical amplification) the collection is enhanced and the gain is higher than one. If the field is reduced (self optical quench) the collection is reduced and the gain becomes lower than one. This optical nonlinearity makes the transducer attractive for optical communications and can be used to distinguish a wavelength, to suppress a color channel or to multiplex or demultiplex an information-modulated wave.

2.3   Frequency analysis

The study of the frequency influence on the device performance was analyzed through the spectral response of the device without and with steady state optical light. Results are displayed in Fig. 4.
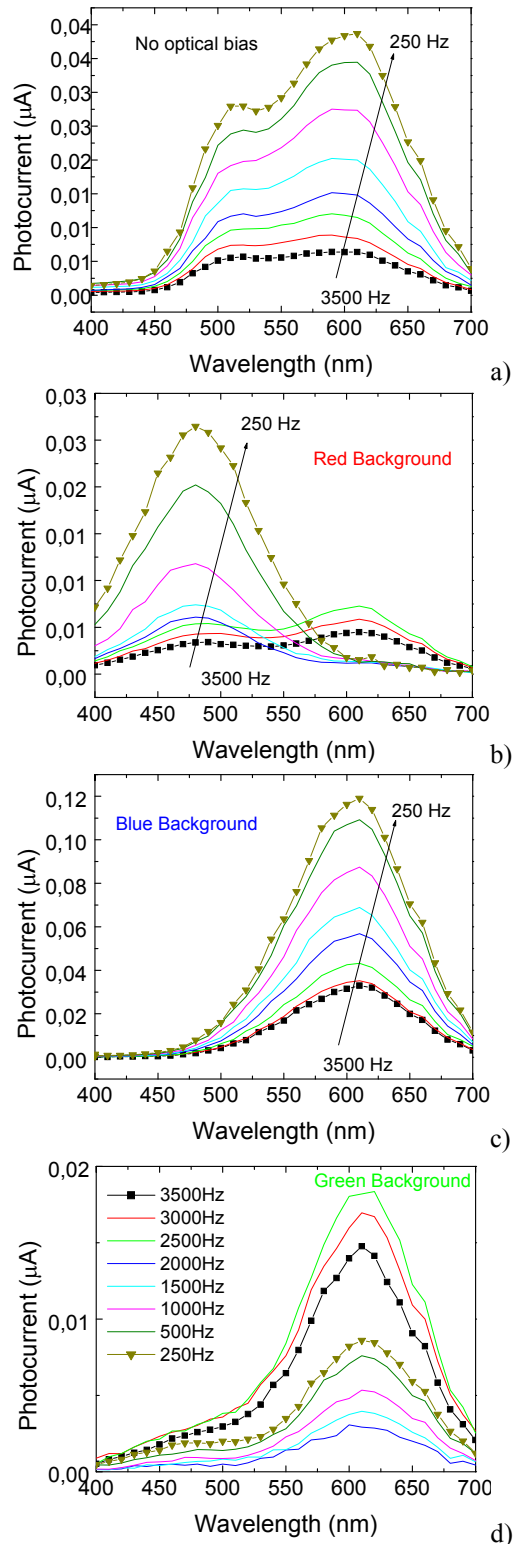
Figure 4   Photocurrent variation with the wavelength for different frequencies at -8 V obtained: a) without, b) with blue, c) with red and d) with green background.

Data from Fig. 4a show that without background light the curves measured under different frequencies exhibit the same trend with two peaks located at 500 nm and 600 nm. The signal is reduced with the increase of the frequency. Under blue steady state illumination (Fig. 4c) the spectral response exhibits a different trend with a single peak located at 600 nm. This is due to the strong attenuation of the short wavelengths. The red steady state illumination (Fig. 4c) has the opposite effect with a single peak at 500 nm. Under green background the spectral response shows two different regimes depending on the operation frequency. In the low frequency range the signal is similar to the trends obtained under red steady state light, while at higher frequencies it follows the behaviour obtained without background light.

Fig. 5 shows the spectral gain as a function of the frequency under red (α^R), green (α^G) and blue (α^B) backgrounds at 624 nm (α_R, red channel), at 526 nm (α_G, green channel) and at 470 nm (α_B, blue channel). Results show how the device reacts to the background wavelength and to the modulated input color channels (pulses) between 250 Hz and 3500 Hz. Under red and green irradiations two frequency regimes can be considered. One, for frequencies lower than 2000 Hz, were either under red and green backgrounds the green and the red channel gains are very low (<<1) and the blue gain is strongly enhanced (>>1) under red background or reduced (<1) under green irradiations. The other regime, for frequencies higher than 2000 Hz, the gain increases with the frequency, gradually under red and quickly under green steady state illumination. Under blue, the gain increases slowly with the frequency being higher than one for the red and green channels and lower for the blue one.

Consequently, under red irradiation (Fig. 5a) the transfer function has extra gain at short wavelengths (blue channel), than at longer wavelengths acting as a short-pass filter whatever the frequency. Under green background (Fig. 5b), the manipulation of amplitude is achieved by changing the frequency of the modulated lights. At high frequencies the device is a band-stop active filter that works to screen out wavelengths that are within a certain range (green channel), giving easy passage only all wavelengths below (blue channel) and above (red channel). In the low frequency regime all the amplitudes are quenched. Under blue steady state optical bias (Fig. 5c) the device behaves as a long-pass active filter that transmits and enhances the long wavelength

photons (red and green channels) while blocking the shorter wavelengths (blue channel).

a)

b)

c)
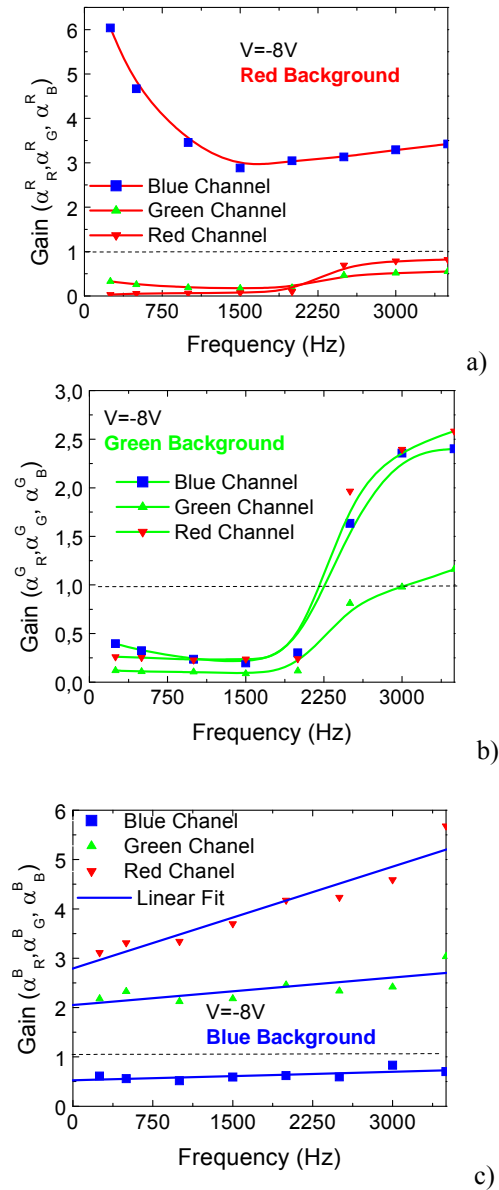
Figure 5   Spectral gain as a function of the frequency at 624 nm (red channel), at 526 nm (green channel) and at 470 nm (blue channel) under red (α^R), green (α^G) and blue (α^B) backgrounds. a) short-pass filter , b) band-stop filter, c) long-pass filter.

3   NUMERICAL SIMULATION

In order to understand the light filtering properties of the device, under different electrical and optical bias conditions, a simulation program ASCA-2D [6]

was used having as input parameters the experimental data. For the a-SiC:H and a-Si:H absorbers an optical band gap of 2.1 eV and 1.8 eV and a thickness of 200 nm and 1000 nm were chosen, respectively. The doping level was adjusted in order to obtain approximately the same conductivity of the typical thin film layers.

a)

b)
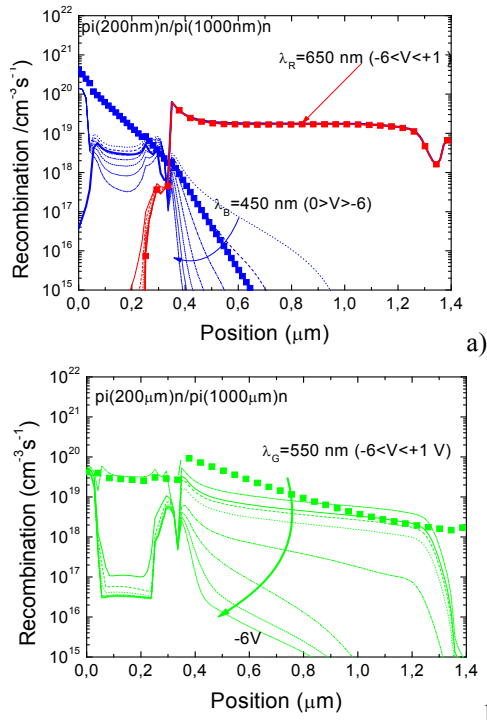
Figure 6   Recombination profiles (straight lines) under: a) red (λ_R =650 nm) and blue (λ_B =450 nm) b) green (λ_G =550 nm) optical bias and different applied voltages. The generation profiles are shown (symbols).

In Fig. 6a the recombination profiles (straight lines) under red (λ_R =650 nm) and blue (λ_B =450 nm) irradiation are displayed at different electrical bias. In Fig 6b it is shown the same profiles but under green bias (λ_G=550 nm). The generation profiles are also displayed (symbols).

Simulated results show that the thickness and the absorption coefficient of the front photodiode are optimized for blue collection and red transmittance, and the thickness of the back one adjusted to achieve full absorption in the greenish region and high collection in the red spectral range. As a result, both front and back diodes act as optical filters confining, respectively, the blue and the red optical carriers, while the green ones are absorbed across both.

Under negative applied voltage, in Fig. 7a it is reported the electric field profile under different

wavelengths backgrounds of the optical bias. In Fig. 7b, under red background, the three red, green and blue channels were added and the electrical field profile displayed.

a)

b)
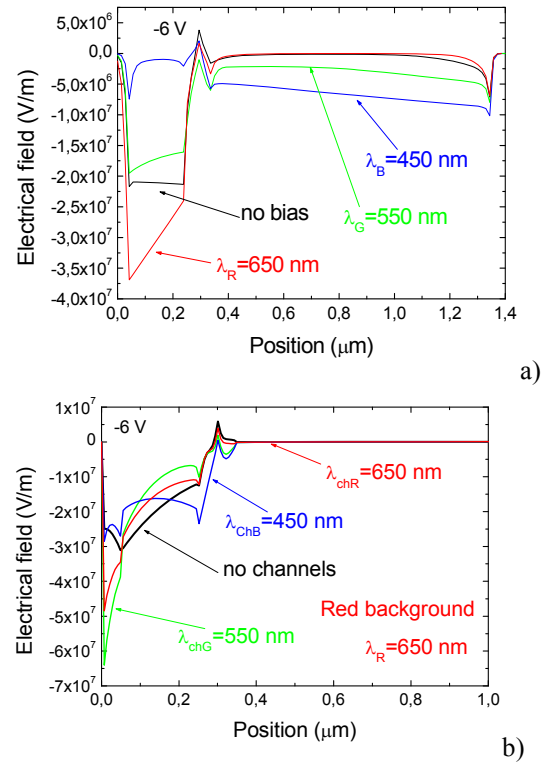
Figure 7   Electric field profiles within the p-i-n/p-i-n tandem structure. a) under different wavelengths backgrounds ($\lambda_{R,G,B}$) and without it. b) red background (λ_R) and different color channels (λ_{chR}, λ_{chG}, λ_{chB})

Results show that the balance between the electrical field adjustments due to the non uniform absorption throughout the structure depends on the generation/recombination ratio profiles at each background wavelength. The shallow penetration of the blue photons into the front diode, the deep penetration of the red photons exclusively into the back diode or the decay of the green absorption across both controls the sensor behavior. The external background interferes mainly with the less absorbing cell (the front under red, the back under blue and with both under green irradiations). Both the front and the back diodes are optically and electrically in series. Under steady state irradiation, to sustain the current across the device, the current at the less absorbing diode has to be adjusted through an increase of the electrical field and thus it becomes reverse biased (Fig. 7a). The superposition of a color

channel will affect locally this field. Under red background (Fig. 7b), the blue channel increases the field intensity in the front diode and even reverse it at the internal interface increasing carrier collection. The red and the green channels change the field in an opposite way.

The sensor is a bias wavelength current-controlled device that makes use of changes in the wavelength of the background to control the power delivered to the load, acting as an amplifier of the optical signals. Its gain (Figs. 3 and 5) depends on the background illumination wavelength. If the electrical field increases locally (self optical amplification) the collection is enhanced and the gain is higher than one. If the field is reduced (self optical quench) the collection is reduced and the gain becomes lower than one [7]. This optical nonlinearity makes the transducer attractive for optical communications and can be used to distinguish a wavelength, to suppress a color channel or to multiplex or demultiplex an information-modulated wave.

4 CAPACITIVE ACTIVE BAND PASS FILTER MODEL

4.1 Two section circuit

Based on the experimental results and device configuration an optoelectronic model supported by the complete dynamical large signal Ebers-Moll model was developed [8, 9] and is displayed in Fig. 8. The electrical model of the device looks fairly complex, but when broken down can be divided into two sections (Fig. 8a): a short-pass filter (front phototransitor, Q_1) and a long-pass filter (back phototransistor, Q_2) sections. So, it can be made out of a short-pass and a long-pass filter when connected both active filter sections in parallel (Fig. 8b).The charge stored in the space-charge layers is modeled by the capacitor C_1 and C_2. R_1 and R_2 model the dynamical resistances of the internal and back junctions under different *dc* bias conditions.

The operation is based upon the following principle: the flow of current through the resistor connecting the two transistor bases is proportional to the difference in the voltages across both capacitors (charge storage buckets).

To allow independent blue, red and green channels transmission four square-wave current sources with different intensities are used; two of them, $\alpha_1 I_1$ and $\alpha_2 I_2$, with different frequencies to simulate the input blue and red channels and the

other two, $\alpha_1 I_3$ and $\alpha_2 I_4$, with the same frequency but different intensities, to simulate the green channel due to its asymmetrical absorption across both front and back phototransistors.
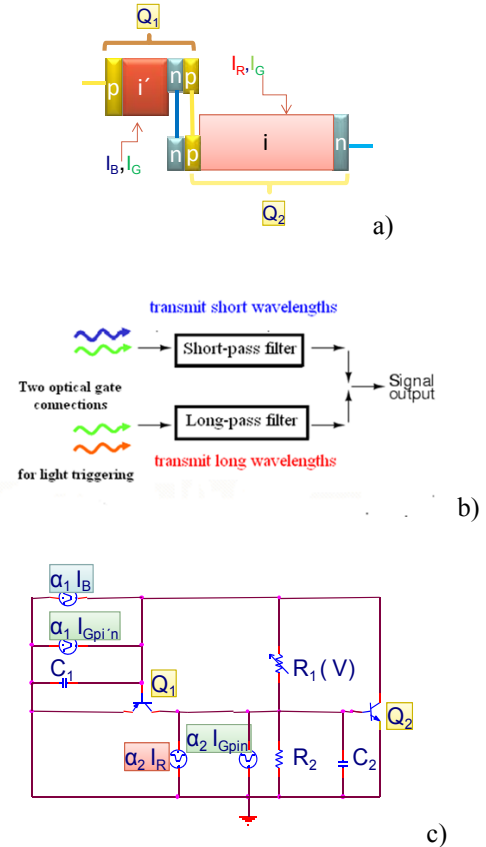
Figure 8   a) Two connected transistor model, b) Two active capacitive filter sections and b) ac equivalent circuit.

Once the *ac* sources are connected in the load loop an *ac* current flows through, establishing voltage modifications across the two capacitors. During the simultaneous transmission of the three independent bit sequences, the set-up in this capacitive circuit loop is constantly changing in magnitude and direction. This means that the voltage across one capacitor builds up until its maximum and the voltage across the other builds up to a minimum. The system collapses and builds up in the opposite direction. It tends to saturate and then leave the saturation because of the cyclic operation. This results in changes on the reactance of both capacitors. The *dc* voltage, according to its strength, aids or opposes the *ac* currents. So, when the pi'npin device is reverse-biased, the base-emitter junction of both transistors are inversely polarized and

conceived as phototransistors, taking, so, advantage of the amplifier action of adjacent collector junctions which are polarized directly. This results in a current gain proportional to the ratio between both collector currents. Under positive bias the internal junction becomes reverse-biased and no amplification effect is observed.

4.2 Optoelectronic state model

Taking into account Fig. 8b the time periodic linearized state equations are given by:

$$\frac{dv_{1,2}}{dt} = \begin{bmatrix} -\dfrac{1}{R_1C_1} & \dfrac{1}{R_1C_1} \\ \dfrac{1}{R_1C_2} & -\dfrac{1}{R_1C_2} - \dfrac{1}{R_2C_2} \end{bmatrix} v_{1,2}(t) + \begin{bmatrix} \dfrac{\alpha_1}{C_1} \\ \dfrac{\alpha_2}{C_2} \end{bmatrix} i_{1,2}(t)$$

$$i(t) = \begin{bmatrix} 0 & \dfrac{1}{R_2} \end{bmatrix} v_{1,2}(t)$$

Where α_1 and α_2 coefficients determine how the background affects the state change. Based on Figs 2-4., under red background, $\alpha_1 > 1$ ($\alpha_B + \alpha_G > 1$) and $\alpha_2 < 1$($\alpha_R + \alpha_G < 1$). The opposite will occur under blue irradiation. Under green background both are balanced.

In Fig. 9 it is displayed the block diagram of the optoelectronic state model for a WDM pí´npin device under different electrical and optical bias conditions. $\lambda_1, \lambda_2, \lambda_3$ represent the color channels, R_1 and R_2 the dynamic internal and back resistances and α_1 and α_2 are the coefficients for the steady state irradiation. To solve the state equations the four order Runge-Kutta method was applied and MATLAB used as a programming environment. The input parameters were chosen in compliance with the experimental results.
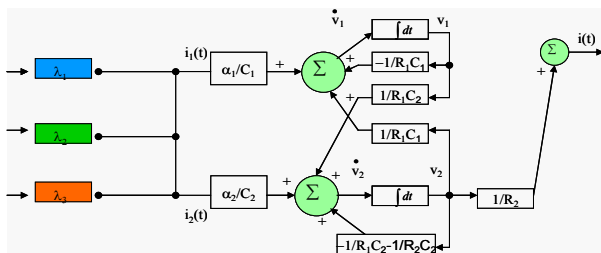
Figure 9   Block diagram of the optoelectronic state model for a pí´n/pin device.

The amplifying elements, α_1 and α_2, can provide gain if needed and attenuate unwanted wavelengths (<1) while amplifying (>1) desired ones. The values

and the strategic placement of the resistors determine the basic shape of the output signals. Under negative bias the device has low ohmic resistance (low R_1) since the base emitter junction of both transistors are reverse polarized and conceived as phototransistors. This results in a charging current gain proportional to the ratio between both collector currents ($\alpha_2 C_1 / \alpha_1 C_2$). Taking into account Figs. 3-4, under red background, $\alpha_1 > 1$ and $\alpha_2 < 1$. The opposite will occur under blue irradiation. Under green background both are balanced. Under positive bias the internal junction becomes reverse-biased and no amplification effect is observed.

4.3 Model validation

Based on the optoelectronic model and experimental results, a multiplexed signal was simulated by applying the Kirchhoff's laws for the *ac* equivalent circuit (Fig. 8c) and the four order Runge-Kutta method to solve the corresponding state equations. MATLAB was used as a programming environment and the input parameters chosen in compliance with the experimental results [7].
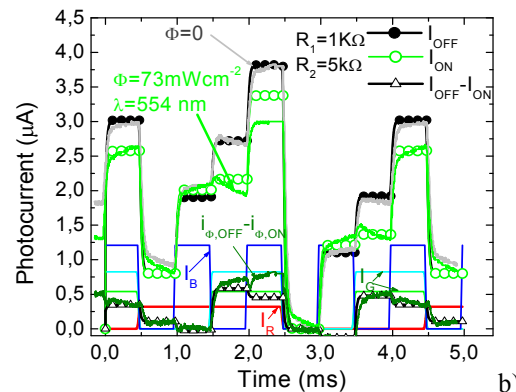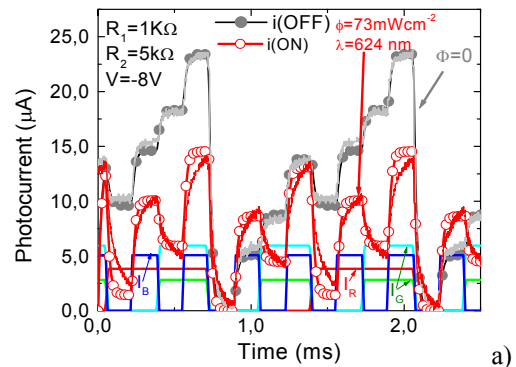
Figure 10   Multiplexed simulated (symbols), current sources (dash lines) and experimental (solid lines) transient responses: under negative *dc* bias and red (a) and green (b) backgrounds.

To simulate the short-pass and ban-stop filters, a multiplexed signal under red and green backgrounds were compared with the correspondent signals without background (symbols). To validate the model the experimental multiplexed signals are shown (solid lines) under the same conditions. The current sources, I_R, I_G, I_B, are also displayed. For their intensity the amplitude of the input experimental channels, without background, were used. To simulate the red and the green backgrounds, current sources intensities were multiplied by the spectral gain ($\alpha_{R,G,B}^{R,G}$) at the correspondent frequency (Fig. 5).

A good agreement between experimental and simulated data was achieved (Fig. 10). As expected, under red background it is observed the enhancement in the short wavelength (red channel) while quenching the longer wavelengths. Under green background the device screens out the medium wavelengths (green channel) and gives a slightly increase on the red and blue wavelengths. Depending on the background wavelength, the device behaves like an optoelectronic controlled transmission system that transmits and/or process intelligence (data) in a manner that permits the subsequent recovery of that information. It filters (amplifies/blocks/screens) the carriers generated by the light pulses (current sources), through the capacitors C_1 and C_2. The manipulation of amplitude is achieved by changing background wavelength at a given modulated frequency. This allows tuning an input channel or to optically demultiplex a polychromatic channel.

5 CONCLUSIONS

A light-activated pi'n/pin a-SiC:H device that combines the demultiplexing operation with the simultaneous photodetection and self amplification of an optical signal is analyzed. A numerical simulation supports the self bias amplification effect.

Results demonstrate that the multiplexed output waveform presents a nonlinear amplitude-dependent response to the wavelengths of the input channels and of the optical bias, acting as an active filter. Depending on the wavelength of the external background it acts either as a short- or a long- pass band filter or as a band-stop filter. A capacitive active band-pass filter model is presented and gives insight into the physics of the device. An algorithm to decode the multiplex signal was established.

REFERENCES

[1] Y.Iguchi et al., *"Novel rear-illuminated 1.55μm – photodiode with high wavelength selectivity designed for bidirectional optical transceiver"*, Proc. 2th Int. Conf. On InP and Related Mater, 317 (2000).

[2] C. Petit, M. Blaser, Workshop on *Optical Components for Broadband Communication* , edited by Pierre-Yves Fonjallaz, Thomas P. Pearsall, Proc. of SPIE Vol. 6350, 63500I, (2006).

[3] M. Vieira, A. Fantoni, M. Fernandes, P. Louro, G. Lavareda, C. N. Carvalho, Journal of Nanoscience and Nanotechnology, Vol. 9, , Number 7, July 2009 , pp. 4022-4027(6).

[4] P. Louro, M. Vieira, Yu. Vygranenko, A. Fantoni, M. Fernandes, G. Lavareda, N. Carvalho, Mat. Res. Soc. Symp. Proc., 989 (2007) A12.04.

[5] M. Vieira, A. Fantoni, P. Louro, M. Fernandes, R. Schwarz, G. Lavareda, and C. N. Carvalho, Vacuum, Vol. 82, Issue 12, 8 August 2008, pp: 1512-1516.

[6] A. Fantoni, M. Vieira, R. Martins, *"Simulation of hydrogenated amorphous and microcrystalline silicon optoelectronic devices"* Mathematics and Computers in Simulation, Vol. 49. pp. 381-401 (1999).

[7] M. Vieira, A. Fantoni, P. Louro, M. Fernandes, R. Schwarz, G. Lavareda, and C. N. Carvalho, *"Self-biasing effect in colour sensitive photodiodes based on double p-i-n a-SiC:H heterojunctions* "Vacuum, Vol. 82, Issue 12, 8 August 2008, pp: 1512-1516.

[8] M. A. Vieira, M. Vieira, M. Fernandes, A. Fantoni, P. Louro, M. Barata, *"Voltage Controlled Amorphous Si/SiC Phototransistors and Photodiodes as Wavelength Selective Devices: Theoretical and Electrical Approaches"* Amorphous and Polycrystalline Thin-Film Silicon Science and Technology — 2009, MRS Proceedings Volume 1153, A08-03.

[9] M. A. Vieira, M. Vieira, J. Costa, P. Louro, M. Fernandes, A. Fantoni, *"Double pin Photodiodes with two Optical Gate Connections for Light Triggering: A capacitive two-phototransistor model"* in Sensors & Transducers Journal Vol. 9, Special Issue, December 2010, pp.96-120.